Journal of Molecular Structure 1311 (2024) 138276

Contents lists available at ScienceDirect

Journal of Molecular Structure

journal homepage: www.elsevier.com/locate/molstr

Assessing indole derivative molecules as dual acetylcholinesterase and butyrylcholinesterase inhibitors through *In Vitro* inhibition and molecular modelling studies

Zuhal Alım [a,*], Hanif Şirinzade [b], Namık Kılınç [c], Esra Dilek [d], Sibel Süzen [e]

[a] Department of Chemistry, Faculty of Arts and Sciences, University of Kırşehir Ahi Evran, 40100, Kırşehir, Turkey
[b] Department of Pharmaceutical Chemistry, Faculty of Pharmacy, Selcuk University, 42130, Konya, Turkiye
[c] Department of Medical Services and Techniques, Vocational School of Health Services, Iğdır University, 76000, Iğdır, Turkey
[d] Department of Biochemistry, Faculty of Pharmacy, Erzincan Binali Yildirim University, Yalnizbag, Erzincan, Turkey
[e] Department of Pharmaceutical Chemistry, Faculty of Pharmacy, Ankara University, 06100, Ankara, Turkiye

ARTICLE INFO

Keywords:
Acetylcholinesterase
Butyrylcholinesterase
Indole derivative
Enzyme inhibition
Molecular docking

ABSTRACT

Alzheimer's Disease (AD) is the most common type of dementia that develops with age, threatens the quality of life, is increases in number around the world, and has no effective treatment. The most important therapeutic targets in drug development studies for the treatment of AD are acetylcholinesterase (AChE) and butyrylcholinesterase (BChE) inhibitors. The inadequacy of existing AChE and BChE inhibitors in the treatment of AD has led to the need to identify new AChE/BChE inhibitors with fewer side effects. In this study, considering the pharmacological importance indole derivatives, inhibition effects of some indole derivative molecules (**a-e**) on AChE and BChE activity were investigated. IC_{50} values of **a-e** against AChE were found to be 0.480 μM, 1.682 μM, 0.916 μM, 1.093 μM, 0.340 μM, respectively. On the other hand, IC_{50} values of compounds **a-e** on BChE activity were determined as 2.18 μM, 4.49 μM, 2.28 μM, 6.36 μM, 1.940 μM, respectively. As a result, it was seen that indole derivatives (**a-e**) showed strong inhibition effect on both enzymes. Additionally, these inhibition results were supported by molecular modelling studies. As a conclusion, results of this study will contribute to studies on the synthesis of new indole-derived AChE and BChE inhibitors for the treatment of AD.

1. Introduction

Alzheimer's Disease (AD) is the most common type of dementia that develops with age, characterized by a decrease in thinking skills, behavioral and cognitive disorders, and progressive memory loss [1–3]. Alzheimer's is the leading cause of death in developing countries [4], and the number of Alzheimer's patients is estimated to reach 107 million in 2050 [2]. AD has been associated with decrease in acetylcholine (ACh) levels [5,6], inflammation in brain cells, accumulation of β-amyloid peptide (Aβ) [7–9] and hyperphosphorylated tau-protein [10–12], neuronal cell death [13], oxidative stress [14], environmental factors and genetic risk [15]. The pathology of AD is quite complex, although many mechanisms have been proposed to explain the pathogenesis of AD, the causes of the disease and appropriate treatment methods are still unclear [6,16]. According to the cholinergic hypothesis, the leading cause of cognitive impairment in AD is thought to be attributed to the decreased ACh levels in the brain [17,18]. ACh plays a potential role in cognitive functions, especially memory. Therefore, the predominant therapeutic agents for AD are inhibitors of cholinesterases (ChEs), such as acetylcholinesterase (AChE) and, by extension, butyrylcholinesterase (BChE); these improve cholinergic neurotransmission in the synaptic cleft by reducing the degradation of ACh [4,19]. AChE inhibitors such as tacrine [20], rivastigmine [21], donepezil [22], galantamine [23], huperzine A [24] have been determined for the treatment of AD. Donepezil, rivastigmine, and galantamine have been approved for use in the treatment of Alzheimer's symptoms [6,25]. Although these approved AChE inhibitors have the effect of improving cognitive disorders and reducing the symptoms of the disease in AD patients, their effects are temporary and do not provide complete recovery [3]. Additionally, these drugs have serious side effects such as hepatoxicity and gastrointestinal discomfort [26]. Therefore, there has been a great need to identify new, effective AChE inhibitors with fewer side effects for the

* Corresponding author at: University of Kırşehir Ahi Evran, Faculty of Arts and Sciences, Department of Chemistry, Kırşehir/Turkey.
E-mail address: zuhal.alim@ahievran.edu.tr (Z. Alım).

https://doi.org/10.1016/j.molstruc.2024.138276
Received 22 January 2024; Received in revised form 4 April 2024; Accepted 5 April 2024
Available online 10 April 2024

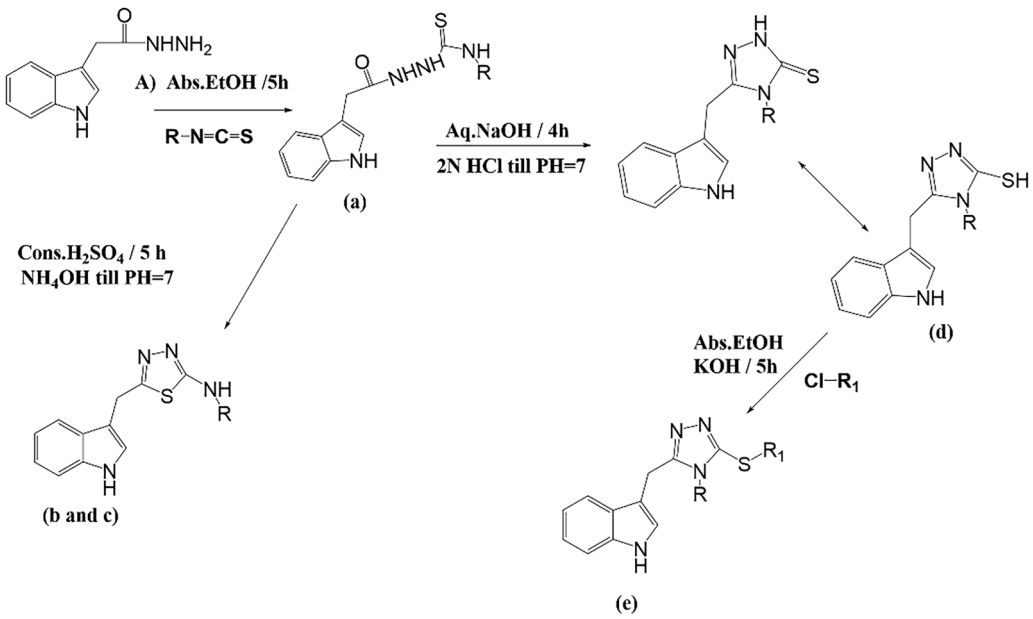

a	b	c	d	e	
R	R	R	R	R	R1

Fig. 1. Molecular structures and synthesis pathway of indole derivative compounds **(a-e).**

treatment of AD. AChE and BChE are sister enzymes that play a key role in cholinergic transmission by hydrolyzing the neurotransmitter acetylcholine [2]. While AChE activity remains unchanged or decreases in the brain of Alzheimer's patients. Additionally it has been observed that BChE activity increases, and the BChE/AChE ratio gradually increase in the brain [3,26]. Recent studies have shown that specific BChE inhibitors improve the cognitive performance of aged rats and other pathological markers of AD in transgenic mice [3,27]. Therefore, the development of not only AChE inhibitors but also specific BChE inhibitors for the treatment of AD has become a topic of increasing interest.

Indole is a heterocyclic compound with two ring systems containing a benzene ring and a pyrrole ring fused to it [28]. It is known as one of the "privileged scaffolds" due to the unique structural motif of the indole ring and can bind with high affinity to various receptors and enzymes [29]. Therefore, indoles are a very valuable class of biochemical compounds that play important roles in the physiological and biochemical processes of living organisms [30]. Indole and indole-based compounds show important biological activities such as anti-inflammatory, anti--microbial, anti-tubercular, anti-cancer, anti-HIV, anti-viral, antioxidant, antimalarial, antidiabetic and anticholinesterase [31]. Indoles are heterocyclic compounds of medical importance that are widely found in the organism.

Pappola et al. [32] was observed that by directing multiple pathologic mechanisms concurrently, certain indoles could be exceptional candidates to improve neurodegeneration. Furthermore, they suggest that controlling of the microbiota to prompt a developed production of neuroprotective indole molecules might support brain well-being through aging. A recent study defined that some indole-based sulfonamide derivatives was found potent having IC_{50} value 0.15 ± 0.050 μM and 0.20 ± 0.10 μM for both AchE and BChE respectively [33]. Similarly novel oxathiolanyl, pyrazolyl and pyrimidinyl indole derivatives exhibited superior inhibitory activity compared with donepezil [34]. In another study, a series of indole derivatives analogous to donepezil was synthesized as acetylcholinesterase inhibitors. 1-(2-(4-(2-fluorobenzyl) piperazin-1-yl) acetyl) indoline-2,3-dione was found to be the most potent [35]. In some studies quinoline–indole derivatives were synthesized and evaluated as multitarget-directed ligands for the treatment of AD [36]. Indole and 7-azaindole derivatives containing, nitrile, piperidine and N-methyl-piperidine substituents at the 3-position prevent the pathological self-assembly of amyloid-β [37]. Novel indole-containing compounds, mainly 3-(2-phenylhydrazono) isatins were synthesized and tested as inhibitors of beta amyloid (Aβ) aggregation. Some of these molecules displayed interesting multitarget activity, by inhibiting monoamine oxidases A and B [38].

In our earlier study, novel indole-based hydrazide/hydrazone derivatives synthesized and established to be possible antioxidant molecules with significant protective effect against amyloid β-induced damage [39]. Most new indole hydrazones were found to have strong antioxidant activities, while they were devoid of inherent cytotoxicity against Chinese hamster ovary (CHO-K1) and rat pheochromocytoma (PC12) cells. In this study, considering the previous data and pharmacological importance of AChE and BChE inhibitors and indole derivatives, inhibition effects of some indole derivative molecules (**a**: 2-(2-(1H-Indol-3-yl)acetyl)-N-phenylhydrazinecarbotioamide, **b**: 5-(1H-Indol-3-yl)methyl)−2-propylamino-1,3,4-thiadiazole, **c**: 5-((1H-Indol-3-yl)methyl)−2-(3-chlorophenyl)amino-1,3,4-thiadiazole, **d**:5-((1H-indol-3-yl)methyl)−4-ethyl-4H-1,2,4-triazole-3-thiol, **e**:2-(5-(1H-Indol-3-yl)methyl)−4-benzyl-4H-1,2,4-triazol-3-ylthio)-N-(2-fluorophenyl) acetamide) on AChE and BChE activity were investigated. Additionally, molecular docking and molecular simulation studies were performed to shed light on inhibition studies.

2. Material and methods

2.1. Materials

Acetylthiocholine iodide (CAS no: 1866–15–5), DTNB (Ellman

reagent, 5,5-dithio-bis-(2-nitrobenzoic acid) (CAS no: 69–78–3) and other chemicals that were used in this study were purchased from Sigma (Germany) and Aldrich (USA). In addition AChE (CAS no. 9000–81–1) and BChE (CAS No. 9001–08–5) was purchased from Sigma-Aldrich.

2.2. Synthesis of indole derivative compounds (a-e)

For the synthesis **a** (Fig. 1) Equal amounts of 2-(1H-indol-3-yl) acetohydrazide (5 mmol) and phenyl isothiocyanate (5 mmol) were dissolved in absolute ethanol (20 ml). The mixture was heated under reflux for 4–5 h at 80–85 °C. The reaction mixture was then concentrated in the rotary evaporator under reduced pressure and kept at room temperature overnight. The crystals thus obtained were purified by washing with petroleum ether [40,41].

2-(2-(1H-Indol-3-yl)acetyl)-N-phenylhydrazincarbothioamide **(a)**: Yield 90 %, m.p. 178.5 C; ^{1}H NMR: 3.63 (s, 2H, COCH2);6.98 (m, 1H, H-5); 7.07 (m, 1H, H-6); 7.26 (d, 1H, J¼ 2.4 Hz, H-2); 7.60 (d, 1H, J¼ 7.6, H-4); 7.14–7.41 (m, 6H, Ar–H); 9.54,9.64, 10.11, 10.91 (s, 4H, NH–NH–CS–NH and NH indole); ^{13}CNMR: 31.17, 108.45, 110.00, 111.75, 118.80, 119.27, 121.44,124.45, 125.44, 126.04, 127.71, 128.55, 136.50, 139.57, 167.71,171.01 (C¼O), 181.33 (S¼C); ESI MS *m/z* 325 (*M* + *H*, 100 %);Anal. calcd. for C17H16N4OS: C, 62.94 %; H, 4.97 %; N, 17.27 %.Found: C, 63.05 %; H, 5.33 %; N, 17.05 %.

In order to synthesis **b** and **c** (Fig. 1), concentrated sulfuric acid (3 ml) was placed in a conical flask, and 5-((1H-Indol-3-yl)methyl)−2-propylamino-1,3,4-thiadiazole and 5-((1H-Indol-3-yl)methyl)−2-(3-chlorophenyl)amino-1,3,4-thiadiazole (1 mmol) was added in small portions over a period of 2 h under stirring while keeping the temperature at 0–5 °C. When the reaction was complete, the mixture was poured into crushed ice and neutralized dropwise with 2 N NH_4OH until the pH was adjusted to 7. The formed precipitate was filtered, washed with water, dried at room temperature and recrystallized from absolute ethanol [40,41].

5-((1H-Indol-3-yl)methyl)−2-propylamino-1,3,4-thiadiazole ***(b)***:Yield 44 %, m.p. 148 C; ^{1}H NMR: 0,86 (t, 3H, J¼ 7.6 Hz,CH3); 1.52 (m, 2H, CH2); 3.15 (q, 2H, NH–CH2); 4.26 (s, 2H, Ar–CH2); 6.98 (t, 1H, J¼ 8 Hz, H-5); 7.09 (t, 1H, J¼ 8 Hz, H-6); 7.31(d, 1H, J¼ 2.4 Hz, H-2); 7.36 (d, 1H, J¼ 8 Hz, H-7); 7.46 (d, 1H,J¼ 8.4 Hz, H-4); 7,82 (s, 1H, NH); 11.00 (s, 1H, NH-indole); ^{13}CNMR: 11.78, 22.16, 26.51, 47.05 (NH–C); 110.91, 112.03, 118.77, 119.12, 121.74, 124.29, 127.01, 136.76, 159.22, 169.06 (N–C–S); ESI MS *m/z* (*M* + *H*, 100 %), 314 (*M* + *H* + CH3CN,100 %); Anal. calcd. for C14H16N4S: C, 51.51 %; H, 6.79 %; N,17.16 %. Found: C, 51.23 %; H, 5.57 %; N, 16.78 %.

5-((1H-Indol-3-yl)methyl)−2-(3-chlorophenyl)amino-1,3,4-thiadiazole ***(c)***: Yield 70 %, m.p. 168 C; ^{1}H NMR: 4.38 (s, 2H, Ar-CH2); 7.10 (m, 1H, H-6); 7.50 (d, 1H, H-4); 6.97–7.88 (m, 7H, Ar-H); 11.04 (s,1H, NH indol); 10.39 (s,1H, NH); ^{13}CNMR: 26.38; 110.92; 112.06; 116.07; 117.03;118.76; 119.17;121.56;121.77; 124.35; 126.95; 131.07; 133.87; 136.77;142.42;162.10; 164.27 (S-C-N); ESI MS *m/z* 341.2 (*M* + *H*,% 100), 343 (*M* + *H* + 2,%45), 382.2 (*M* + *H*+CH3CN,%38); Anal. calcd. for C14H16N4S: C, 55.51 %; H, 4.38 %; N,15.23 %. Found: C, 55.22 %; H, 4.09 %; N, 15.34 %.

For the synthesis **d** (Fig. 1), 2-(1H-Indol-3-yl-acetyl)-N-Ethyl hydrazincarbothioamide (2 mmol) and 2 N NaOH solution (25 ml) were placed in conical flask. The mixture was heated under reflux for 4–5 h. The reaction mixture was then neutralized dropwise with 2 N HCl untill the pH was adjusted to 7. The precipitate thus obtained was filtered, washed with water and recrystallized from a mixture of ethanol/water (4:1) [40,41].

5-((1H-Indol-3-yl)methyl)−4-ethyl-4H-1,2,4-triazole-3-thiol ***(d)***: Yield 91 %, m.p. 191.5 C; ^{1}H NMR: 0.92 (t, 3H, J¼ 7.6 Hz,CH3); 3.90 (q, 2H, CH2); 4.20 (s, 2H, Ar–CH2); 6.98 (dt, 1H,J1 ¼ 7.2, J2 ¼ 0.8 Hz, H-5); 7.09 (dt, 1H, J1 ¼ 7.2, J2 ¼ 1.2 Hz H-6); 7.33 (d, 1H, J¼ 2.4 Hz, H-2); 7.37 (d, 1H, J¼ 8 Hz, H-7); 7.49(d, 1H, J¼ 7.6 Hz, H-4); 11.05 (s, 1H, NH indole); 13.54 (s, 1H,SH); ^{13}C NMR: 13.31; 22.34; 38.72; 107.70; 112.057; 118.73;119.16; 121.76; 124.61; 127.14; 136.70; 151.70; 166.67 (N–C–S);ESI MS *m/z* 259 (*M* + *H*, 100 %), 300 (*M* + *H* + CH3CN, 8 %);Anal. calcd. for C13H14N4S: C, 57.63 %, H, 5.73 %, N, 20.68 %. Found: C, 57.93 %, H, 5.96 %, N, 20.51 %.

Finally, in the **e** synthesis (Fig. 1), 5-((1H-Indol-3-yl) methyl)−4-ethyl-4H-1,2,4-triazole-3-thiol (1 mmol) was dissolved in a solution of 2 N KOH (2 ml) and absolute ethanol (20 ml) in a conical flask. 2-chloro-N-(2-fluorophenyl) acetamide (1 mmol) was added in to the mixture and stirred at room temperature for 2–3 h. After completion of the reaction, the mixture was poured onto crushed ice. The resulting precipitate was filtered, washed with water, dried at room temperature and recrystallized from absolute ethanol [41,42].

2-(5-((1H-Indol-3-yl)methyl)−4-benzyl-4H-1,2,4-triazole-3-ylthio)-N-(2fluorophenyl) acetamide ***(e)***: Yield 30 %, m.p.182.5 C; ^{1}H NMR: 4.13(s, 2H, indole-CH2); 4.20 (s, 2H,benzyl-CH2); 5.18 (s, 2H, amide-CH2); 6.92–7.88 (m, 14H,Ar-H); 10.16 (s, 1H, amide-NH); 10.91 (s, 1H, NH-indole); ^{13}CNMR: 22.20; 37.64 (S–C); 47.02 (N–C); 108.48; 111.89;115.87; 116.07; 118.98; 121.67; 124.09; 124.25; 124.87; 125.86;126.27; 126.38; 127.02; 127.22; 128.20; 129.08; 135.832; 136.76;149.86; 152.56; 155.00; 155.46; 166.82 (C¼O); ESI MS*m/z* 472.2 (*M* + *H*, 100 %); Anal. calcd. for C26H22 FN5OS:C, 66.22 %, H, 4.70 %, N, 14.85 %. Found: C, 65.73 %, H, 5.08% N, 14.36 %.

2.3. Activity assays of AChE and BChE

In this study, AChE activity measurement was performed according to a spectrophotometric method of Ellman et al. [43]. The basis of this method is as follows: Acetylthiocholine iodide used as substrate. AChE hydrolyzes acetylthiocholine to thiocholine and acetic acid. The thiocholine formed as a result of the reaction reacts with the DTNB (Ellman reagent, 5,5-dithio-bis-(2-nitrobenzoic acid) used in the reaction medium to form 5-thio-2-nitrobenzoic acid, a yellow compound. The color intensity of the resulting compound is monitored for 3 min as an increase in absorbance at 412 nm using a spectrophotometer. This change in absorbance is due to the formation of 5-thio-2-nitrobenzoic acid from the reaction of thiocholine with DTNB. The rate of change in absorbance is proportional to AChE activity. The enzyme unit was calculated using the molar absorption coefficient (13.600 $M^{-1}.cm^{-1}$) of 5-thio-2-nitrobenzoic acid at 412 nm [44]. On the other hand, BChE is another enzyme involved in cholinergic neurotransmission, and its activity is measured spectrophotometrically by the Ellman method, similar to AChE activity. In other words, here too, the hydrolysis of butyrylthiocholine iodide substrate by BChE and the formation of green 5-thio-2--nitrobenzoate anion as a result of the reaction of thiocholine with DTNB are monitored with a spectrophotometer at 412 nm [45].

2.4. In vitro inhibition studies on AChE and BChE

AChE (CAS no. 9000-81-1) and BChE (CAS No. 9001-08-5) used in the study were purchased from Sigma-Aldrich. The inhibitory effects of indole derivatives (**a-e**) on AChE and BuChE activities were determined by IC_{50} values under *in vitro* conditions. IC_{50} refers to the inhibitor concentration that reduces the enzyme activity by half, and a low IC_{50} value indicates high inhibition power. To determine the IC_{50} values of **a-e** molecules, AChE and BChE activities were measured at least five different concentrations of each **a-e** molecules and% Activities were calculated. The control activity of the enzymes was accepted as 100 %. Inhibitor concentrations were then plotted against% Activity for each molecule. From these graphs, the IC_{50} values of each molecule for AChE and BuChE were determined.

2.5. In silico studies

2.5.1. Homology modelling

Since the three-dimensional structure of equine serum BChE has not been experimentally solved, homology modeling was performed for this enzyme. The amino acid sequence of equine BChE was obtained from the

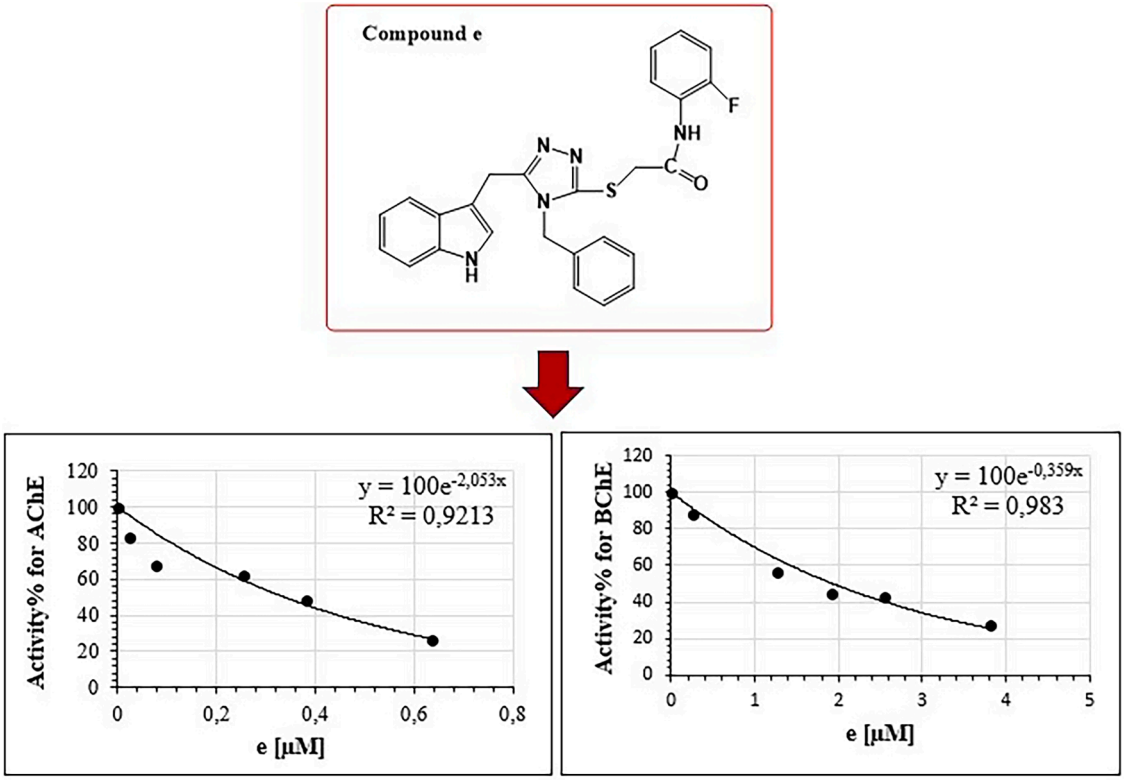

Fig. 2. Compound **e** and IC_{50} graphs showing strong inhibitory effects on AChE and BChE.

UniProt Knowledgebase (entry: P81908) and used as input for the protein homology modeling process. The Prime Homology Modeling module was employed to create a comparative model of equine serum BChE. This modeling process utilized the high-resolution crystal structure of full-length, recombinant human BChE (PDB ID: 4TPK) as a template for generating the equine BChE model. Prime combines homology modeling and fold recognition in a single integrated tool. Additionally, it offers the flexibility for expert users to fine-tune and customize various parameters, thus enhancing the accuracy and effectiveness of the predictions [46,47].

2.5.2. *Molecular docking*

In silico studies were conducted to investigate the interaction between indole derivatives and AChE and BChE enzymes through Induced-fit molecular docking simulations [48] as detailed in our previous studies [49–51]. The simulations were carried out using Maestro 12.5, a component of the Schrödinger Molecular Modeling Suite software [52]. The crystal structure of the AChE receptor, identified by its PDB ID: 4TVK, was acquired from the RCSB Protein Data Bank. Conversely, the crystal structure of the BChE receptor was constructed using homology modeling, utilizing the template with PDB ID: 4TPK. Both receptors were prepared at physiological pH using the Protein Preparation Wizard [53]. Optimization and minimization of the receptors were performed using the OPLS3e force field. A receptor grid was generated around the natural ligands in the protein structures. The ligands were prepared and protonated at pH 7.0 ± 2.0 using the LigPrep module.

2.5.3. *Calculation of binding free energy using molecular mechanics/generalized born surface area (MM-GBSA)*

To calculate the binding free energies (ΔG_{bind}), the Molecular Mechanics/Generalized Born Surface Area (MM/GBSA) method was employed. This method combines continuum solvation models with molecular mechanics computations to estimate the binding free energies of protein-ligand complexes. The Prime/MM-GBSA calculations utilized the OPLS3e force field and the VSGB dissolvable model [54].

2.5.4. *ADME studies*

ADME studies were performed to better understand the pharmacokinetic properties, drug-likeness, and physicochemical characteristics of indole derivatives (**a, b, c, d,** and **e**). The absorption, distribution, metabolism, and excretion properties of these indole derivatives were analyzed using the QikProp panel in Maestro 12.5. QikProp provides information by comparing the properties of a novel molecule to those of 95 % of known drugs. This analysis helps evaluate drug-likeness and predict the potential behavior of the indole derivatives in terms of their absorption, distribution, metabolism, and excretion.

2.5.5. *Molecular dynamics simulations*

Molecular dynamics simulations were carried out using the Desmond software from D. E. Shaw Research [55]. According to the results of molecular docking, the compound with the highest binding score against both enzymes was selected and combined with the corresponding enzyme. The protein-ligand complex was prepared using the Desmond system builder module and positioned in the center of an orthorhombic box with a 10 Å buffer zone around the protein. To create a solvated and neutral system, water molecules (Tip3p) and counter ions (NaCl at 0.15 M) were added. The system underwent energy minimization using the OPLS4 force field. The complex was then loaded into the Desmond molecular dynamics module, and a simulation of 50 ns duration was performed under constant temperature (300 K) and pressure (1 bar) conditions using default parameters. The simulation employed a time step of 2.5 fs and the RESPA integrator. The interactions between the ligand and protein during binding were analyzed, along with the calculation of the Root Mean Square Deviation (RMSD) of the protein's Cα atoms and the ligand's heavy atoms, using Desmond.

Table 1
The IC_{50} values for **a-e** compounds on AChE and BChE.

Compounds	IC_{50} for AChE	IC_{50} for BChE
a	0.480 μM	2.18 μM
b	1.682 μM	4.49 μM
c	0.916 μM	2.28 μM
c	1.093 μM	6.36 μM
e	0.340 μM	1.94 μM
Tacrine*	57,9 nM	3,19 nM

* Tacrine was used as standard inhibitor for AChE and BChE.

3. Results and discussion

AD is a neurodegenerative disorder that is becoming more common with the aging population worldwide. The Alzheimer's Association estimates that unless effective treatment methods are found, the disease could reach over 100 million worldwide by 2050. The adverse effects of AD can place a significant burden on healthcare systems [56]. Therefore, conducting studies on the development of effective treatment methods for AD is a very important need today. AChE and BChE are enzymes that play a vital role in cholinergic transmission by hydrolyzing the neurotransmitter acetylcholine [17]. Acetylcholine plays an important role in the cognitive functions of the brain, and therefore the impairment of cognitive functions due to Alzheimer's is associated with Acetylcholine deficiency [18]. Because of AD association with cholinergic loss, cholinesterase inhibitors are the most effective and well-established strategy for treating AD [57]. To date, many cholinesterase inhibitors have been developed for the treatment of AD, but their inability to fully treat the disease and their side effects have [3,26] led to the need to discover new inhibitors that have fewer side effects and are more effective against the disease. In recent years, pharmacological studies on the treatment of AD have focused on research based on multiple targets with a single drug, and this has been shown to be effective for the treatment of AD [58,59]. In the light of this information, the inhibition effects of indole-derived molecules (**a-e**) on both AChE and BChE activities were investigated in this study.

The inhibitory effects of compounds **a-e** on AChE and BChE activity were determined by IC_{50} (inhibitor concentration that halves the activity) values. For AChE, IC_{50} values of molecules **a-e** were found to be 0.480 μM, 1.682 μM, 0.916 μM, 1.093 μM, 0.340 μM, respectively. According to these results, the compound showing the strongest inhibitory effect on AChE activity was compound **e**. On the other hand, IC_{50} values showing the inhibition effects of compounds **a-e** on BChE activity were determined as 2.18 μM, 4.49 μM, 2.28 μM, 6.36 μM, 1.940 μM, respectively. Compound **e** had the strongest inhibitory effect for BChE as well as AChE (Fig. 2). Inhibition results are summarized in Table 1. Tacrin was used as the reference inhibitor for both enzymes. When the inhibition results were compared with tacrine, it was seen that the indole molecules we used in this study were less effective inhibitors than tacrine. However, the inhibitory effects of indole molecules on AChE and BChE were at micromolar levels. In addition, our results showed that compounds **a-e** had a stronger inhibitory effect for AChE than for BChE.

In this investigation, molecular modeling methodologies were employed to elucidate the potential inhibitory mechanisms of indole derivatives known for their experimentally validated dual inhibition effects on AChE and BChE enzymes. The study aimed to distinguish the complex interactions between these compounds and the enzymes. To achieve this goal, a comprehensive array of in silico techniques was applied, including molecular docking, MM-GBSA, ADME analysis, molecular dynamics, and homology modeling methods.

Within the context of homology modeling, the model created by the Prime module was presented as a ribbon representation in the workspace. The final model was automatically annotated with two distinct colors to indicate their respective significance. Specifically, residues that were identical to the template were colored blue, while similar residues were highlighted in cyan. Sequence insertions are colored appropriately as shown in Fig. 3.

Fig. 3. 3D model of the protein obtained by homology modeling.

Subsequently, it is essential to assess the quality of the model and address any identified issues, such as steric clashes, deviations in bond lengths and angles, and other structural anomalies. The Protein Preparation Wizard provides a valuable tool to effectively rectify common structural problems. The sequence identity of the equine serum BChE enzyme, when compared to the 4TVK crystal structure used as a template, was found to be 90 %. Additionally, the positivity rate was determined to be 94 %.

The model produced using the Prime module in Schrodinger Maestro underwent evaluation through a Ramachandran plot, which allows visualization of residues positioned within specific regions of the phi/psi space. In the plot, residues residing within the allowed regions were depicted in yellow, those in favored regions appeared in reddish-orange, while residues falling into disallowed regions were represented in white. Notably, Fig. 4 illustrates that the majority of residues were found within the allowed regions, while only a negligible number of residues were situated in disallowed regions. ERRAT and Verify3D online models were also used for further validation of the protein structure obtained as a result of homology modeling. The data derived from Verify3D analysis reveals that 89.27 % of the residues exhibit an average 3D-1D score of $>= 0.1$. Furthermore, following the ERRAT analysis, the Overall Quality Factor of the homology-modeled protein was determined to be 92.88 (Supplementary Figs. 1, 2, and 3). These results indicate a high level of structural accuracy for the modeled protein [60–62].

We employed the Induced-Fit Docking (IFD) methodology to conduct molecular docking studies using indole derivatives to gain a better knowledge of the protein-ligand interactions at the atomic level **a, b, c, d**, and **e**, which have strong inhibitory effects on AChE and BChE enzymes, were subjected to the Induced-fit docking protocol. As positive control substance, tacrine, a standard inhibitor of both AChE and BChE enzymes, was utilized. In addition, we utilized the Prime MM/GBSA module to quantify free binding energies to truly comprehend the thermodynamic variables involved in the AChE and BChE inhibitory actions of **a, b, c, d**, and **e**. Table 2 summarizes the IFD docking scores and Prime/MM-GBSA values.

Compound **e** demonstrated the most potent inhibitory activity against AChE and BChE enzymes among the indole compounds tested, as evidenced by its lowest IC_{50} value. The results from molecular docking studies for **e** consistently support the experimental data. Significantly, the induced-fit docking simulations yielded remarkably high docking

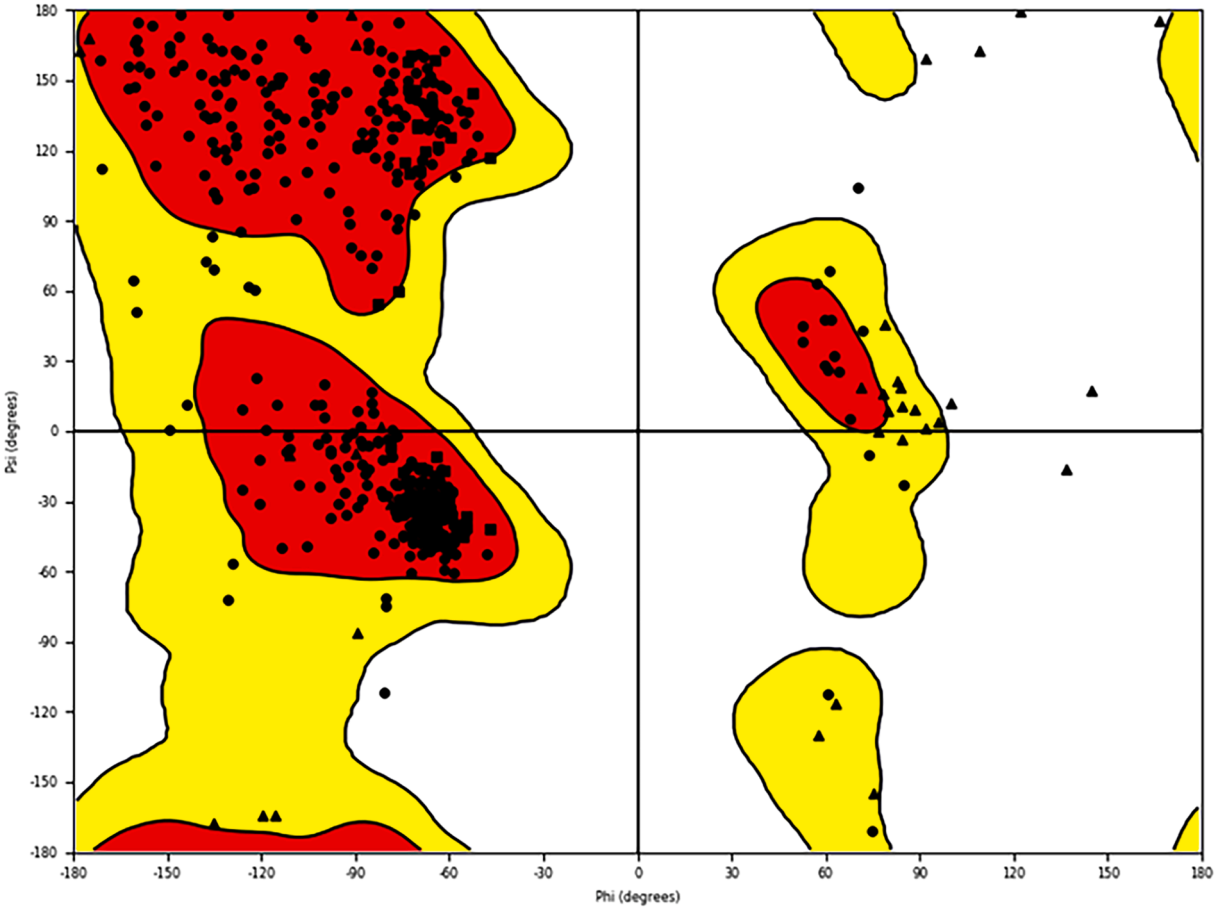

Fig. 4. Ramachandran plot of the modelled protein.

Table 2
IFD docking scores, and Prime/MM-GBSA free binding energy results of the indole compounds that show potent enzyme inhibitory activity.

Compound	AChE		BChE	
	IFD Docking Score (kcal/mol)	MM-GBSA ΔG_{bind} (kcal/mol)	IFD Docking Score (kcal/mol)	MM-GBSA ΔG_{bind} (kcal/mol)
a	−11.112	−55.06	−10.649	−49.11
b	−10.093	−34.98	−9.818	−47.17
c	−11.061	−33.38	−10.788	−47.30
d	−10.413	−30.43	−9.385	−27.67
e	−12.240	−96.91	−12.925	−83.73
Tacrine	−13.570	−75.45	−9.873	−58.58

scores of −12.240 kcal/mol for the AChE enzyme and −12.925 kcal/mol for the BChE enzyme, underscoring the strong binding affinity between the compounds and the respective enzymes. Moreover, the MM-GBSA analysis demonstrated a calculated free binding energy of −96.91 kcal/mol and −83.73 kcal/mol, respectively, further highlighting the strong and robust interaction between compound **e** and the AChE and BChE enzymes (Table 2).

In the active site of the AChE enzyme, compound **e** formed hydrogen bonds with specific amino acid residues, namely ASP72, TYR121, PHE288, and ARG289. Additionally, compounds **e** engaged in pi-pi interactions with TYR70, PHE290, PHE330, and PHE331, critical components situated in the active site of the AChE enzyme (Fig. 5**A**). In the active site of the BChE enzyme, compound **e** formed hydrogen bonds with specific amino acid residues, namely GLY116, GLY117, ALA328, and HIS438. Additionally, compound **e** engaged in pi-pi interactions with TRP82, PHE329, and TYR332 (Fig. 5**B**). These observations provide confirmation that compound **e** effectively occupies the active sites of both the AChE and BChE enzymes, exerting a potent inhibitory effect through its extensive and substantive interactions.

Molecular docking studies were conducted on compound **a**, which exhibited a remarkably potent experimental inhibition effect against both AChE and BChE enzymes, second only to compound **e**. These computational investigations further confirmed the validity of the experimental findings. Notably, the induced-fit docking simulations resulted in remarkably high docking scores of −11.112 kcal/mol for the AChE enzyme and −10.649 kcal/mol for the BChE enzyme, indicating a profound binding affinity between the compounds and the respective enzymes. Additionally, the MM-GBSA analysis revealed calculated free binding energies of −55.06 kcal/mol and −49.11 kcal/mol, respectively, further emphasized the strong and robust interaction between compound **a** and the AChE and BChE enzymes (Table 2).

Compound **a** demonstrated hydrogen bonding with specific amino acid residues, including ASP72, GLH199, SER200, and HIS440, within the active site of the AChE enzyme. Additionally, it engaged in pi-pi interactions with TRP84 and PHE330, crucial components situated in the AChE enzyme's active site (Fig. 3). Similarly, within the BChE enzyme's active site, compound **a** formed hydrogen bond with particular amino acid residue, namely HIS438, and participated in pi-pi interactions with TRP82, TRP231, and PHE329 (Fig. 3).

Molecular docking and molecular mechanics studies were carried out for compounds **b, c,** and **d**, which exhibited pronounced *in vitro* inhibition effects against AChE and BChE enzymes in experimental assays. The computational analyses further corroborated and validated the experimental data for these compounds.

To assess the drug-likeness and pharmacokinetic attributes of the

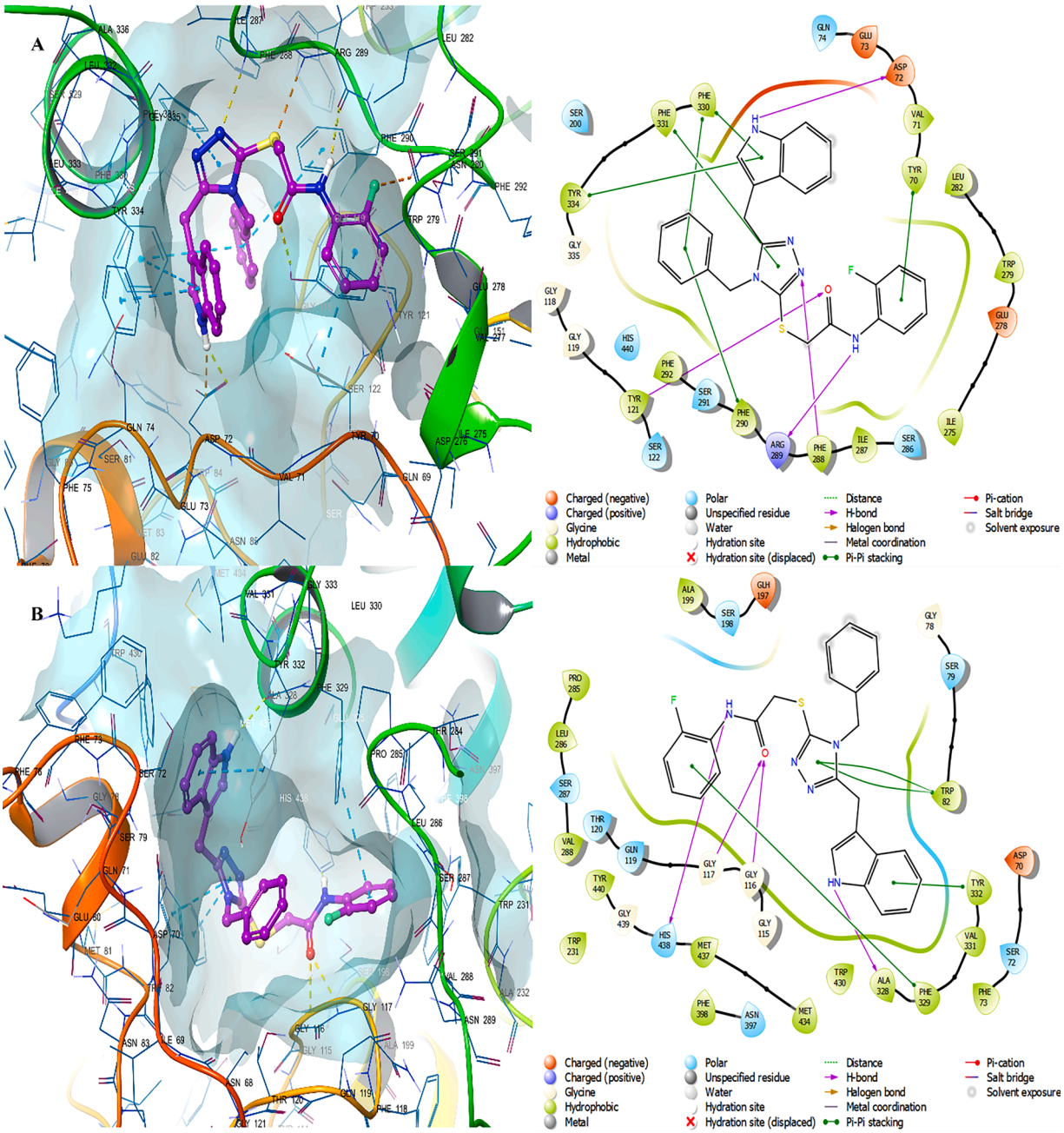

Fig. 5. The detailed 3D docking pose (on the left) and the corresponding 2D ligand-receptor interaction diagram (on the right) of compound **e** for both AChE (A) and BChE (B) receptors.

indole compounds, we utilized the QikProp tool from Maestro. This analysis aimed to evaluate the compounds' potential as viable drugs based on their physicochemical and pharmaceutical characteristics. The molecular weight (mol MW), the number of hydrogen bonds accepted (acceptHB), and the number of hydrogen bonds donated (donorHB) values of the compounds were found to be within acceptable ranges. Additionally, we utilized the QPPCaco factor, which ranged from 634,647 to 1790,066, to assess the potential apparent Caco-2 cell permeability in nm/*sec*. Cell permeability through biological membranes is a crucial factor in drug development. Furthermore, the

Table 3
The evaluation of ADME (Absorption, Distribution, Metabolism, and Excretion) prediction results for the indole compounds.

Compound	mol MW	donorHB	acceptHB	QPlogPo/w	QPlogS	QPlogHERG	QPPCaco	QPlogBB	QPPMDCK	%HOA	RuleOfFive	RuleOfThree
a	324,4	3,25	4,25	3342	−5052	−6471	634,647	−0,836	542,749	96,671	0	0
b	272,367	2	2,5	3603	−4,51	−5263	1608,985	−0,438	1370,446	100	0	0
c	340,829	2	2,5	4,59	−5652	−5926	1375,319	−0,296	2519,185	100	0	0
d	258,34	1,8	2	3393	−3861	−4514	1790,066	−0,187	2216,853	100	0	0
e	471,551	2	4,5	5916	−6876	−6965	794,747	−0,938	829,737	100	1	1
Tacrine	198,267	1,5	2	2,56	−3071	−4067	2851,902	0,032	1535,666	100	0	0

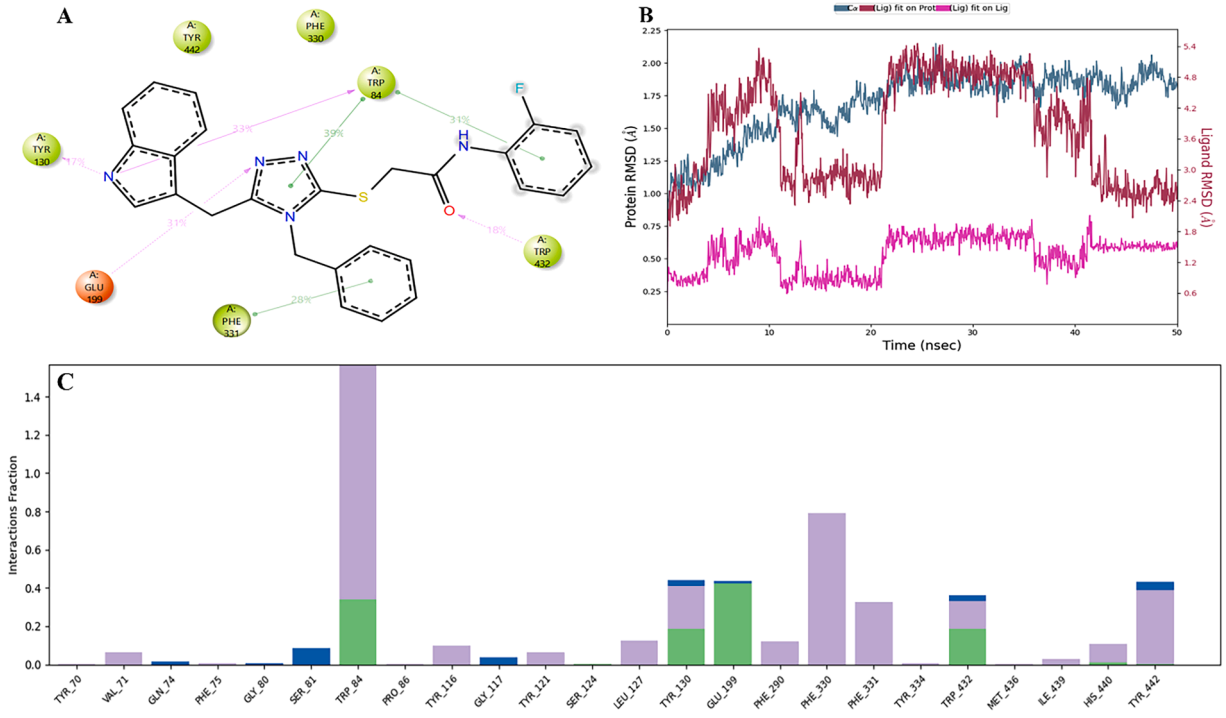

Fig. 6. The MD simulation analysis of compound **e** in complex with AChE was conducted, and the results are presented as follows: **A**) The key protein-ligand interactions, which occurred for more than 15.0 % of the simulation time, are highlighted. **B**) The protein Cα RMSD (pale blue) is plotted on the left y-axis, while the ligand RMSD fit (red) on the protein is shown on the right y-axis. The 'Lig fit Lig' RMSD (pink) represents the ligand's deviation from its reference conformation. **C**) Interaction fraction histograms showcase the ligand's interactions with each of the key residues of the protein.

octanol/water partition coefficients (QPlogPo/w) of all compounds were observed to be high (ranging from 3342 to 5916), indicating favorable drug dispersion and absorption characteristics. The QPlogPo/w values are indicative of the lipophilic nature of potential drug candidates and their solubility in lipid-based environments. The compounds' water solubility (QPlogS) values ranged from −3861 to −6876,

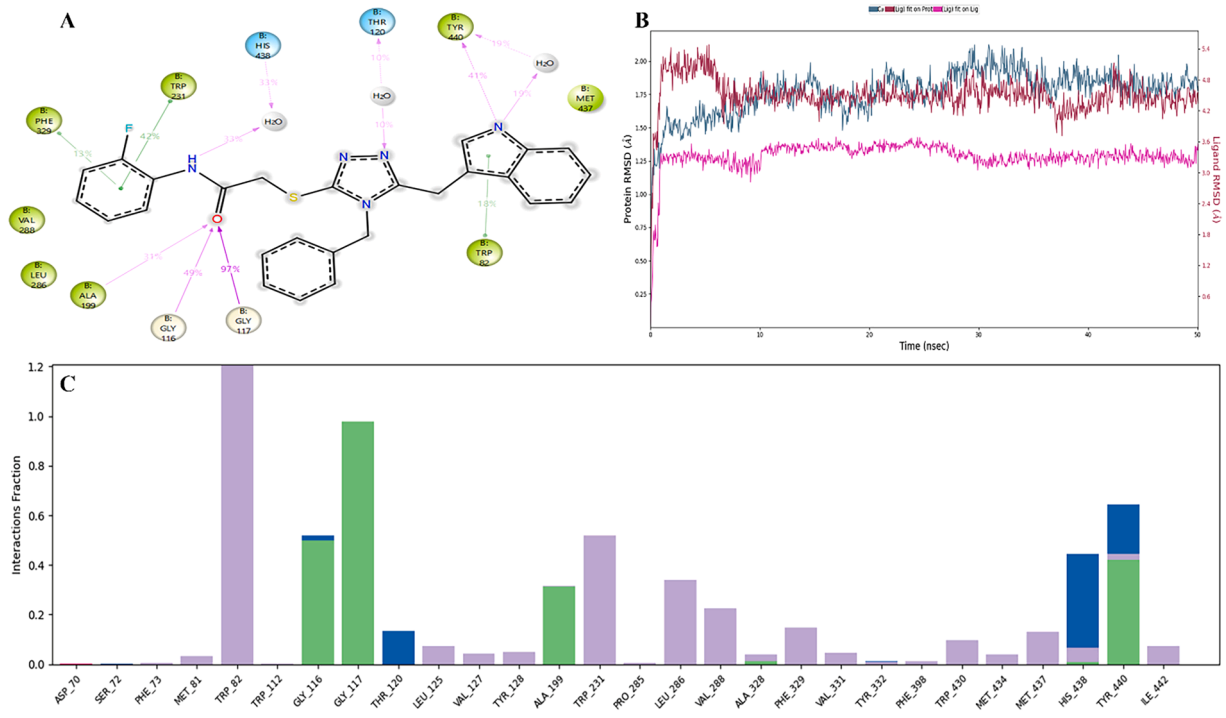

Fig. 7. The compound **e** was subjected to MD simulation analysis in complex with BChE, and the obtained results are presented as follows: **A**) The significant protein-ligand interactions, which persisted for more than 10.0 % of the simulation time, are highlighted. **B**) The plot displays the protein Cα RMSD (pale blue) on the left y-axis, while the ligand RMSD fit (red) on the protein is shown on the right y-axis. The 'Lig fit Lig' RMSD (pink) represents the ligand's variation from its reference conformation. **C**) Interaction fraction histograms illustrate the ligand's interactions with each key residue of the protein.

and their cell-permeable parameter (QPPMDCK) values ranged from 542,749 to 2519,185, while their K^+ channel blockage (QPlogHERG) values were less than −5 (except for 1d). Moreover, the compounds displayed percentages of human oral absorption (%HOA) values between 96,671 and 100 %. Notably, the QPlogBB parameter assessed the compounds' ability to pass the blood-brain barrier, suggesting their potential utility in treating neurological disorders. Specifically, compound **e**, identified as a potent inhibitor of AChE and BChE enzymes involved in neurological illnesses, exhibited a QPlogBB value within the recommended range. Overall, all the compounds met the pharmacokinetic criteria for drug-like substances and were well within the clinically acceptable range (Table 3). These findings indicate their promising potential as drug candidates.

In order to assess the stability of the ligand-protein complex and identify key interactions, molecular dynamics simulation studies were conducted specifically for compound **e**, given its exceptional in vitro inhibition, docking score, and significant MM-GBSA binding free energy results. Figs. 5 and 6 illustrate the results of the molecular dynamics simulation analysis for the complex of compound **e** with AChE and BChE, respectively.

Fig. 6**A** illustrates the hydrogen bond interactions (indicated by the purple arrow) of compound **e** with TRP84 (33 % of simulation time), TYR130 (17 % of simulation time), GLU199 (31 % of simulation time), and TRP432 (18 % of simulation time) within the active site of the AChE enzyme. Furthermore, compound **e** forms dual pi-pi stacking interactions (shown by the green line) with TRP84 (31 % and 39 % of simulation time, respectively) and a single pi-pi interaction with the PHE331 residue (28 % of simulation time).

Fig. 6**B** displays the ligand and protein RMSD plots. The average protein Cα RMSD value was determined as about 2.8 Å (pale blue), the average ligand fit on protein RMSD value as about 2 Å (red), and the 'Lig fit Lig' RMSD value was measured at about 1 Å (pink).

Fig. 6**C** presents the interaction fraction histograms, depicting the ligand's interactions with key residues of the protein during the 50-nanosecond simulation. Hydrogen bond interactions are represented by green columns, hydrophobic interactions by purple columns, and water-bridged hydrogen bond interactions by blue columns.

Fig. 7**A** illustrates the hydrogen bond interactions (indicated by the purple arrow) of compound **e** with GLY116 (49 % of simulation time), GLY117 (97 % of simulation time), ALA199 (31 % of simulation time), and TYR440 (41 % of simulation time), within the active site of the BChE enzyme. Compound **e** exhibited additional hydrogen bond interactions with residues THR120, TYR440, and HIS438, facilitated by water molecules. Furthermore, compound **e** forms pi-pi stacking interaction (shown by the green line) with TRP82 (18 % of simulation time), TRP231 (42 % of simulation time) and PHE329 residue (13 % of simulation time).

Fig. 7**B** displays the ligand and protein RMSD plots. The average protein Cα RMSD value was determined as about 2.7 Å (pale blue), the average ligand fit on protein RMSD value as about 3 Å (red), and the 'Lig fit Lig' RMSD value was measured at about 1 Å (pink).

Fig. 7**C** presents the interaction fraction histograms, depicting the ligand's interactions with key residues of the protein during the 50-nanosecond simulation. Hydrogen bond interactions are represented by green columns, hydrophobic interactions by purple columns, and water-bridged hydrogen bond interactions by blue columns.

4. Conclusion

In drug development studies targeting therapeutic agents for AD are focusing on AChE and BChE inhibitors, that aim to alleviate acetylcholine loss. The deficiencies observed in existing inhibitors for AD underscore the necessity of identifying novel and effective AChE and BChE inhibitors. This study elucidates the inhibitory effects of indole molecules a-e on AChE and BChE activities, with in vitro inhibition results confirmed by molecular modeling studies. The findings presented herein are anticipated to make significant contributions to the synthesis of novel indole-derived AChE and BChE inhibitors, thereby advancing therapeutic avenues for Alzheimer's disease.

CRediT authorship contribution statement

Zuhal Alım: Writing – review & editing, Writing – original draft, Visualization, Validation, Investigation, Formal analysis, Data curation. **Hanif Şirinzade:** Writing – review & editing, Writing – original draft, Validation, Methodology, Investigation. **Namık Kılınç:** Writing – original draft, Validation, Methodology, Investigation. **Esra Dilek:** Writing – original draft, Validation, Formal analysis. **Sibel Süzen:** Writing – review & editing, Writing – original draft, Methodology, Investigation.

Declaration of competing interest

No potential conflict of interest was reported by the authors.

Data availability

Data will be made available on request.

Acknowledgments

The authors thank to Kırşehir Ahi Evran University Research Fund Accounting for their support to carry out this work (Project number: FEF. A4. 23. 013).

Supplementary materials

Supplementary material associated with this article can be found, in the online version, at doi:10.1016/j.molstruc.2024.138276.

References

[1] S. Karantzoulis, J.E. Galvin, Distinguishing Alzheimer's disease from other major forms of dementia, Expert Rev. Neurother. 11 (2011) 1579–1591, https://doi.org/10.1586/ern.11.155.
[2] M. Taha, F. Rahim, N. Uddin, F.U. Ullah, N. Iqbal, E.H. Anouar, M. Salahuddin, R. K. Farooq, M. Gollapalli, K.M. Khan, A. Zafar, Exploring indole-based-thiadiazole derivatives as potent acetylcholinesterase and butyrylcholinesterase enzyme inhibitors, Int. J. Biol. Macromol. 188 (2021) 1025–1036, https://doi.org/10.1016/j.ijbiomac.2021.08.065.
[3] H. Ullah, F. Rahim, H. Zada, S. Hayat, F. Khan, M.S. Khan, Synthesis, molecular docking, and bioactivity study of isoquinoline-sulfonamide hybrid analogues: a promising acetylcholinesterase and butyrylcholinesterase inhibitor candidate, Chem. Data Collect. 46 (2023) 101048, https://doi.org/10.1016/j.cdc.2023.101048.
[4] N.E.H. Hammoudi, W. Sobhi, A. Attoui, T. Lemaoui, A. Erto, Y. Benguerba, In silico drug discovery of Acetylcholinesterase and Butyrylcholinesterase enzymes inhibitors based on quantitative structure-activity relationship (QSAR) and drug-likeness evaluation, J. Mol. Struct. 1229 (2021) 129845, https://doi.org/10.1016/j.molstruc.2020.129845.
[5] A.V. Terry, J. Buccafusco, The cholinergic hypothesis of age and Alzheimer's disease-related cognitive deficits: recent challenges and their implications for novel drug development, JPET 306 (2003) 821–827, https://doi.org/10.1124/jpet.102.041616.
[6] Pesaresi A, Lamba D, Vezenkov L, D. Tsekova, V. Lozanov, Kinetic and structural studies on the inhibition of acetylcholinesterase and butyrylcholinesterase by a series of multitarget-directed galantamine-peptide derivatives, Chem. Biol. Interact. 365 (2022) 110092, https://doi.org/10.1016/j.cbi.2022.110092.
[7] J. Busciglio, D.H. Gabuzda, P. Matsudaira, Generation of beta-amyloid in the secretory pathway in neuronal and nonneuronal cells, PNAS 90 (1993) 2092–2096, https://doi.org/10.1073/pnas.90.5.2092.
[8] M.P. Murphy, H. LeVine, Alzheimer's disease and the b-Amyloid peptide, J. Alzheimer's Dis. 19 (2010) 311, https://doi.org/10.3233/JAD-2010-1221.
[9] D.A. Butterfield, A.M. Swomley, R. Sultana, Amyloid β-Peptide (1–42)-Induced oxidative stress in Alzheimer disease: importance in disease pathogenesis and progression, Antioxid. Redox Signal. 19 (2012) 823–835, https://doi.org/10.1089/ars.2012.5027.
[10] G. Lippens, A. Sillen, I. Landrieu, et al., Tau aggregation in Alzheimer's disease, Prion 1 (2007) 21–25, https://doi.org/10.4161/pri.1.1.4055.

[11] K. Iqbal, F. Liu, C.X. Gong, Tau in Alzheimer disease and related tauopathies, Curr. Alzheimer Res. 7 (2010) 656–664, https://doi.org/10.2174/156720510793611592.
[12] G. Simic, M.B. Leko, S. Wray, C. Harrington, I. Delalle, N. Jovanov-Milosevic, D. Bazadona, L. Buee, R. De Silva, G. Di Giovanni, C. Wischik, P.R. Hof, Tau Protein Hyperphosphorylation and aggregation in Alzheimer's disease and other tauopathies, and possible neuroprotective strategies, Biomolecules 6 (2016) 6, https://doi.org/10.3390/biom6010006.
[13] P. Goel, S. Chakrabarti, K. Goel, K. Bhutani, T. Chopra, S. Bali, Neuronal cell death mechanisms in Alzheimer's disease: an insight, Front. Mol. Neurosci. 15 (2022) 937133, https://doi.org/10.3389/fnmol.2022.937133.
[14] W.J. Huang, X. Zhang, W.W. Chen, Role of oxidative stress in Alzheimer's disease (Review), Biomed. Rep. 4 (2016) 519–522, https://doi.org/10.3892/br.2016.630.
[15] R.J. Boyd, D. Avramopoulos, L.L. Jantzie, A.S. McCallion, Neuroinfammation represents a common theme amongst genetic and environmental risk factors for Alzheimer and Parkinson diseases, J. Neuroinflammation. 19 (2022) 223, https://doi.org/10.1186/s12974-022-02584-x.
[16] L. Fan, C. Mao, X. Hu, S. Zhang, Z. Yang, Z. Hu, H. Sun, Y. Fan, Y. Dong, J. Tang, C. Shi, Y. Xu, New insights into the pathogenesis of Alzheimer's disease, Front. Neurol. 10 (2020) 1312, https://doi.org/10.3389/fneur.2019.01312.
[17] S. Khan, H. Ullah, R. Hussain, Y. Khan, M.U. Khan, M. Khan, A. Sattar, M.S. Khan, Synthesis, in vitro bio-evaluation, and molecular docking study of thiosemicarbazone-based isatin/bis-schiff base hybrid analogues as effective cholinesterase inhibitors, J. Mol. Struct. 1284 (2023) 135351, https://doi.org/10.1016/j.molstruc.2023.135351.
[18] E. Scarpini, P. Scheltens, H. Feldman, Treatment of Alzheimer's disease; current status and new perspectives, Lancet Neurol. 2 (2003) 539–547, https://doi.org/10.1016/S1474-4422(03)00502-7.
[19] N.H. Greig, T. Utsuki, Q.S. Yu, X. Zhu, H.W. Holloway, T. Perry, B. Lee, D. K. Ingram, D.K. Lahiri, A new therapeutic target in Alzheimer's disease treatment: attention to butyryloholinesterase, Curr. Med. Res. Opin. 17 (2001) 159–165, https://doi.org/10.1185/0300799039117057.
[20] J.S. Kelly, Alzheimer's disease: the tacrine legacy, Trends Pharmacol. Sci. 20 (1999) 127–129, https://doi.org/10.1016/S0165-6147(99)01344-9.
[21] B.R. Williams, A. Nazarians, M.A. Gill, A review of rivastigmine: a reversible cholinesterase inhibitör, Clin. Ther. 25 (2003) 1634–1653, https://doi.org/10.1016/s0149-2918(03)80160-1.
[22] S. Akasofu, M. Kimura, T. Kosasa, K. Sawada, H. Ogura, Study of neuroprotection of donepezil, a therapy for Alzheimer's disease, Chem. Biol. Interact. 175 (2008) 222–226, https://doi.org/10.1016/j.cbi.2008.04.045.
[23] M. Gauding, U. Richarz, J. Han, B.V. Baelen, B. Schauble, Effects of galantamine in Alzheimer's Disease: double-blind withdrawal studies evaluating sustained versus interrupted treatment, Curr. Alzheimer Res. 8 (2011) 771–780, https://doi.org/10.2174/156720511797633205.
[24] H.Y. Zhang, C.Y. Zheng, H. Yan, Z.F. Wang, L.L. Tang, X. Gao, X.C. Tang, Potential therapeutic targets of huperzine A for Alzheimer's disease and vascular dementia, Chem. Biol. Interact. 175 (2008) 396–402, https://doi.org/10.1016/j.cbi.2008.04.049.
[25] M. Mehta, A. Adem, M. Sabbagh, New acetylcholinesterase inhibitors for Alzheimer's disease, Int. J. Alzheimers Dis. 2012 (2012) 728983, https://doi.org/10.1155/2012/728983.
[26] H. Ullah, M. Jabeen, F. Rahim, A. Hussain, F. Khan, M. Perviaz, M. Sajid, I. Uddin, M.U. Khan, M. Nabi, Synthesis, acetylcholinesterase and butyrylcholinesterase inhibitory potential and molecular docking study of thiazole bearing thiourea analogues, Chem. Data Collect. 44 (2023) 100988, https://doi.org/10.1016/j.cdc.2022.100988.
[27] N.H. Greig, T. Utsuki, D.K. Ingram, Y. Wang, G. Pepeu, C. Scali, Q.S. Yu, J. Mamczarz, H.W. Holloway, T. Giordano, D. Chen, Selective butyrylcholinesterase inhibition elevates brain acetylcholine, augments learning and lowers Alzheimer β-amyloid peptide in rodent, PANAS 102 (2005) 17213–17218, https://doi.org/10.1073/pnas.0508575102.
[28] D.F. Taber, P.K. Tirunahari, Indole synthesis: a review and proposed classification, Tetrahedron 67 (2011) 7195–7210, https://doi.org/10.1016/j.tet.2011.06.040.
[29] F.R. De Sa Alves, E.J. Barreiro, C.A.M. Fraga, From Nature to drug discovery: the indole scaffold as a privileged structure, Mini Rev. Med. Chem. 9 (2009) 782–793, https://doi.org/10.2174/138955709788452649.
[30] N.K. Kaushik, N. Kaushik, P. Attri, N. Kumar, C.H. Kim, A.K. Verma, E.H. Choi, Biomedical importance of indoles, Molecules 18 (2013) 6620–6662, https://doi.org/10.3390/molecules18066620.
[31] S. Kumar, A. Ritika, A brief review of the biological potential of indole derivatives, Future J. Pharm. Sci. 6 (2020) 121, https://doi.org/10.1186/s43094-020-00141-y.
[32] M.A. Pappolla, G. Perry, X. Fang, M. Zagorski, K. Sambamurti, B. Poeggeler, Indoles as essential mediators in the gut-brain axis. Their role in Alzheimer's disease, Neurobiol. Dis. 156 (2021) 105403, https://doi.org/10.1016/j.nbd.2021.105403.
[33] Z.A. Homoud, M. Taha, F. Rahim, N. Iqbal, M. Nawaz, R.K. Farooq, A. Wadood, M. Alomari, I. Islam, S. Algheribe, A.U. Rehman, K.M. Khan, N. Uddin, Synthesis of indole derivatives as Alzheimer inhibitors and their molecular docking study, J. Biomol. Struct. Dyn. 41 (2023) 9865–9878, https://doi.org/10.1080/07391102.2022.2148126.
[34] E.M. Azmy, I.F. Nassar, M. Hagras, I.M. Fawzy, M. Hegazy, M.M. Mokhtar, A. M. Yehia, N.S. Ismail, W.H. Lashin, New indole derivatives as multitarget anti-Alzheimer's agents: synthesis, biological evaluation and molecular dynamics, Future Med. Chem. 15 (2023) 473–495, https://doi.org/10.4155/fmc-2022-0228.
[35] M.M. Ismail, M.M. Kamel, L.W. Mohamed, S.I. Faggal, Synthesis of new indole derivatives structurally related to donepezil and their biological evaluation as acetylcholinesterase inhibitors, Molecules 17 (2012) 4811–4823, https://doi.org/10.3390/molecules17054811.
[36] Z. Wang, J. Hu, X. Yang, X. Feng, X. Li, L. Huang, A.S.C. Chan, Design, synthesis, and evaluation of orally bioavailable quinoline-indole derivatives as innovative multitarget-directed ligands: promotion of cell proliferation in the adult murine hippocampus for the treatment of Alzheimer's disease, J. Med. Chem. 61 (2018) 1871–1894, https://doi.org/10.1021/acs.jmedchem.7b01417.
[37] N. Sreenivasachary, H. Kroth, P. Benderitter, A. Hamel, Y. Varisco, D.T. Hickman, W. Froestl, A. Pfeifer, A. Muhs, Discovery and characterization of novel indole and 7-azaindole derivatives as inhibitors of β-amyloid-42 aggregation for the treatment of Alzheimer's disease, Bioorg. Med. Chem. Lett. 27 (2017) 1405–1411, https://doi.org/10.1016/j.bmcl.2017.02.001.
[38] R. Purgatorio, N. Gambacorta, M. Catto, M. De Candia, L. Pisani, A. Espargaro, R. Sabate, S. Cellamare, O. Nicolotti, C.D. Altomare, Pharmacophore Modeling and 3D-QSAR Study of Indole and Isatin Derivatives as Antiamyloidogenic Agents Targeting Alzheimer's Disease, Molecules 25 (2020) 5773, https://doi.org/10.3390/molecules25235773.
[39] H. Gurer-Orhan, C. Karaaslan, S. Ozcan, O. Firuzi, M. Tavakkoli, L. Saso, S. Suzen, Novel indole-based melatonin analogues: evaluation of antioxidant activity and protective effect against amyloid β-induced damage, Bioorg. Med. Chem. 24 (2016) 1658–1664, https://doi.org/10.1016/j.bmc.2016.02.039.
[40] N. Siddiqui, M.S. Alam, W. Ahsan, Synthesis, anticonvulsant and toxicity evaluation of 2-(1H-indol-3-yl) acetyl-N-(substituted phenyl) hydrazine carbothioamides and their related heterocyclic derivatives, Acta Pharmaceut. 58 (2008) 445–454, https://doi.org/10.2478/v10007-008-0025-0.
[41] H. Shirinzadeh, E. Ince, A.D. Westwell, H.G. Orhan, S. Suzen, Novel indole-based melatonin analogues substituted with triazole, thiadiazole and carbothioamides: studies on their antioxidant, chemopreventive and cytotoxic activities, J. Enzyme Inhib. Med. Chem. 31 (2016) 1312–1321, https://doi.org/10.3109/14756366.2015.1132209.
[42] C. Orek, P. Koparir, M. Koparir, N-cyclohexyl-2-[5-(4-pyridyl)-4-(p-tolyl)-4H-1,2,4-triazol-3-ylsulfanyl]-acetamide dihydrate: synthesis, experimental, theoretical characterization and biological activities, Spectrochim. Acta A Mol. Biomol. Spectrosc. 97 (2012) 923–934, https://doi.org/10.1016/j.saa.2012.07.082.
[43] G.L. Ellman, K.D. Courtney, V. Andres, R.M. Featherstone, A new andrapid colorimetric determination of acetylcholinesterase activity, Biochem. Pharmacol. 7 (1961) 88–90, https://doi.org/10.1016/0006-2952(61)90145-9.
[44] H. Shirinzade, E. Dilek, Z. Alım, Evaluation of Naphthalenylmethylen hydrazine derivatives as potent inhibitors on, Antiatherogenic enzymes, Paraoxonase i and acetylcholinesterase activities, ChemistrySelect 7 (2022) e202104489, https://doi.org/10.1002/slct.202104489.
[45] I. Gulcin, A. Scozzafava, C.T. Supuran, Z. Koksal, F. Turkan, S. Çetinkaya, Z. Bingöl, Z. Huyut, S.H. Alwasel, Rosmarinic acid inhibits some metabolic enzymes including glutathione *S*-transferase, lactoperoxidase, acetylcholinesterase, butyrylcholinesterase and carbonic anhydrase isoenzymes, J. Enzyme Inhib. Med. Chem. 31 (2016) 1698–1702, https://doi.org/10.3109/14756366.2015.1135914.
[46] M.P. Jacobson, D.L. Pincus, C.S. Rapp, T.J.F. Day, B. Honig, D.E. Shaw, R. A. Friesner, A hierarchical approach to all-atom protein loop prediction, Proteins: Struct., Funct., Bioinf 55 (2004) 351–367, https://doi.org/10.1002/prot.10613.
[47] Schrödinger Release 2020–3, Prime, Schrödinger, LLC, New York, NY, 2020.
[48] W. Sherman, T. Day, M.P. Jacobson, R.A. Friesner, R. Farid, Novel procedure for modeling ligand/receptor induced fit effects, J. Med. Chem. 49 (2006) 534–553, https://doi.org/10.1021/jm050540c.
[49] A. Akıncıoğlu, S. Göksu, A. Naderi, H. Akıncıoğlu, N. Kılınç, I. Gulçin, Cholinesterases, carbonic anhydrase inhibitory properties and in silico studies of novel substituted benzylamines derived from dihydrochalcones, Comput. Biol. Chem. 94 (2021) 107565, https://doi.org/10.1016/j.compbiolchem.2021.107565.
[50] N. Gök, A. Akıncıoğlu, E.B.E.H. Akıncıoğlu, N. Kılınç, S. Göksu, Synthesis of novel sulfonamides with anti-Alzheimer and antioxidant capacities, Arch. Pharm. 354 (2021) e2000496, https://doi.org/10.1002/ardp.202000496.
[51] N. Kılınç, U. Güller, Z. Alım, Identification of the inhibition effects of some natural antiproliferative agents on CA-I, CA-II, and AChE activities isolated from human erythrocytes by kinetic and molecular docking studies, Russ. J. Bioorganic Chem. 48 (2022) 720–730, https://doi.org/10.1134/S1068162022040124.
[52] Schrödinger Release 2020–3: Maestro, Schrödinger, LLC, New York, NY, 2020.
[53] G.M. Sastry, M. Adzhigirey, T. Day, R. Annabhimoju, W. Sherman, Protein and ligand preparation: parameters, protocols, and influence on virtual screening enrichments, J. Comput. Aided Mol. Des. 27 (2013) 221–234, https://doi.org/10.1007/s10822-013-9644-8.
[54] S. Genheden, U. Ryde, The MM/PBSA and MM/GBSA methods to estimate ligand-binding affinities, Expert Opin. Drug Discov. 10 (2015) 449–461, https://doi.org/10.1517/17460441.2015.1032936.
[55] K.J. Bowers, E. Chow, H. Xu, R.O. Dror, M.P. Eastwood, B.A. Gregersen, J. L. Klepeis, I. Kolossvary, M.A. Moraes, F.D. Sacerdoti, J.K. Salmon, Y. Shan, D. E. Shaw, Scalable algorithms for molecular dynamics simulations on commodity clusters, in: Proceedings of the ACM/IEEE Conference on Supercomputing (SC06), Tampa, Florida, 2006, https://doi.org/10.1145/1188455.1188544.
[56] L. Mucke, Neuroscience: alzheimer's disease, Nature 461 (2009) 895–897, https://doi.org/10.1038/461895a.
[57] A. Nordberg, A.L. Svensson, Cholinesterase inhibitors in the treatment of Alzheimer's disease, Drug Saf. 19 (1998) 465–480, https://doi.org/10.2165/00002018-199819060-00004.
[58] R. Leon, A.G. Garcia, J. Marco-Contelles, Recent advances in the multitargetdirected ligands approach for the treatment of Alzheimer's disease, Med. Res. Rev. 33 (2013) 139–189, https://doi.org/10.1002/med.20248.

[59] M. Rosini, Polypharmacology: the rise of multitarget drugs over combination therapies, Future Med. Chem. 6 (2014) 485–487, https://doi.org/10.4155/fmc.14.25.
[60] C. Colovos, T.O. Yeates, Verification of protein structures: patterns of nonbonded atomic interactions, Protein Sci. 2 (1993) 1511–1519, https://doi.org/10.1002/pro.5560020916.
[61] J.U. Bowie, R. Lüthy, D. Eisenberg, A method to identify protein sequences that fold into a known three-dimensional structure, Science 253 (1991) 164–170, https://doi.org/10.1126/science.1853201.
[62] R. Luthy, J.U. Bowie, D. Eisenberg, Assessment of protein models with three-dimensional profiles, Nature 356 (1992) 83–85, https://doi.org/10.1038/356083a0.